Australasian Physical & Engineering Sciences in Medicine (2019) 42:619–626
https://doi.org/10.1007/s13246-019-00737-6

TECHNICAL PAPER

Dose verification for liver target volumes undergoing respiratory motion

Emma Dyce[1] · Dean Cutajar[2] · Peter Metcalfe[2] · Simon Downes[1]

Received: 13 July 2018 / Accepted: 19 February 2019 / Published online: 2 May 2019

Abstract

Respiratory motion has a significant impact on dose delivered to abdominal targets during radiotherapy treatment. Accurate treatment of liver tumours adjacent to the diaphragm is complicated by large respiratory movement, as well as differing tissue densities at the lung–liver interface. This study aims to evaluate the accuracy of dose delivered to superior liver tumours using passive respiratory monitoring, in the absence of gating technology, for a range of treatment techniques. An in-house respiratory phantom was designed and constructed to simulate the lung and liver anatomy. The phantom consisted of adjacent slabs of lung and liver equivalent materials and a cam drive system to emulate respiratory motion. A CC04 ionisation chamber and Gafchromic EBT3 film were used to perform point dose and dose plane measurements respectively. Plans were calculated using an Elekta Monaco treatment planning system (TPS) on exhale phase study sets for conformal, volume modulated arc therapy (VMAT) and intensity modulated radiation therapy (IMRT) techniques, with breathing rates of 8, 14 and 23 bpm. Analysis confirmed the conformal delivery protocol currently used for this site within the department is suitable. The experiments also determined that VMAT is a viable alternative technique for treatment of superior liver lesions undergoing respiratory motion and was superior to IMRT. Furthermore, the measurements highlighted the need for respiratory management in these cases. Displacements due to respiration exceeding planned margins could result in reduced coverage of the clinical target volume and much higher doses to the lung than anticipated.

Keywords Liver · 4D · IGRT · Respiratory motion

Introduction

Liver cancer incidence is currently on the rise in many countries, including Australia, predominantly due to increasing hepatitis C infections [1], with men and the elderly at the greatest risk. Mortality rates are also comparatively high, with the Australian 5-year relative survival rate from 2007 to 2011 at just 16% [2]. While the standard treatment regime for hepatocellular carcinoma (HCC) and oligometastatic disease within the liver involves surgical resection or liver transplantation, non-surgical alternatives including external beam radiotherapy (EBRT) are options for inoperable tumours [3]. Despite recent advances in radiotherapy, HCC lesions still pose a significant treatment challenge, due to very large tumour sizes, motion of the tumour due to respiration, and the high likelihood of radiation induced liver disease. For successful local control without serious hepatic toxicities, high, conformal doses must be delivered to the target while simultaneously sparing healthy hepatic tissue. There is currently much discussion in the literature for the optimal method of achieving this dosimetric outcome [4, 5].

Research has showed that use of simple, conformal techniques such as parallel opposed beam pairs are ineffectual in controlling HCC primary tumours of the liver. Whole liver irradiation has also been shown to result in high acute and late hepatic toxicity, including radiation-induced liver disease [6]. Conformal radiotherapy using multiple additional beams allows dose escalation to the planning target volume (PTV) to reduce the risk of recurrence, while simultaneously reducing dose to surrounding healthy liver tissue, thereby reduce toxicity effects. Recent international guidelines including National Comprehensive Cancer Network guidelines for hepatobiliary cancers [7] recommend EBRT

✉ Emma Dyce
emma.dyce@health.nsw.gov.au

[1] Nelune Comprehensive Cancer Centre, Prince of Wales Hospital, Sydney, Australia

[2] Centre for Medical Radiation Physics, University of Wollongong, Wollongong, Australia

as a locoregional treatment for unresectable HCC lesions, with a particular focus on stereotactic body radiation therapy (SBRT) [8]. Lesions close to the diaphragm, as investigated in this project, are an indication for SBRT [9].

Using intensity modulated radiation therapy (IMRT) techniques has been shown by Thomas et al. [10] to offer improved treatment plans for liver tumours when compared to conformal plans with the same conventional fractionation schemes. As there exists a large variability amongst patients with liver cancers in terms of tumour location, distance of the tumour to OARs, the total volume of the liver and the number of tumour sites, standard beam arrangements may prove inadequate and a superior plan can often be achieved with IMRT [11]. IMRT allows for shaping of the isodose curves to reduce the dose delivered to organs at risk, and in the cases that the liver itself is the dose limiting structure, the ability to vary dose delivered across the target may increase the allowable target dose, particularly for small tumour sites [10].

The aim of the project was to evaluate the use of 3D conformal, IMRT and VMAT techniques for the treatment of HCC in the superior region of the liver, for different rates of respiration. This was achieved by measuring the disagreement between calculated and delivered dose caused by respiratory motion effects (including interplay) near a liver–lung interface in a custom-made respiratory phantom. This study examines the different treatment techniques used in conjunction with Active Breathing Control (ABC) (Elekta, Sweden) and in the absence of gating or tracking technology.

Materials and methods

Custom respiratory phantom

An in-house phantom was designed and built specifically for use in this project. The primary design criteria were to replicate the lung–liver interface of an adult patient using tissue-equivalent materials and to simulate respiratory motion in the superior–inferior direction. The largest movement of liver tumours is in this direction and caused predominantly by respiration [12]. Movements of up to 8 cm have been observed in the liver [13], however an average displacement appears to be 1–2 cm with at least some movement observed in most patients [14]. The motion was designed to emulate a standard non-sinusoidal breathing pattern, with approximately even inhale-exhale ratio and a pause in the exhale position. The breathing pattern was based on patient traces acquired with the RPM system. The phantom was to have an adjustable 'breathing rate' and a cavity for an ionisation chamber detector. A CC04 ionisation chamber (IBA Dosimetry, Germany), volume 0.04 cm^3, was used to obtain point-dose measurements. EBT3 Gafchromic film (Ashland, USA) was used to obtain high-spatial resolution 2-dimensional dose planes, from which 1D dose profiles could be extracted.

The phantom is comprised of two adjacent slabs of materials emulating the lung and liver, cut such that film can be placed near isocentre in the coronal plane. The lung slab has dimensions 19 cm (left–right) by 7 cm (superior–inferior) by 10 cm (anterior–posterior) and was constructed from cedar wood. The liver slab was constructed from Gammex 457 Solid Water (Gammex, Inc, USA) and has an additional 3 cm length in the superior–inferior direction. Each section is held together by vertical plastic rods. Three metal spheres of diameter 2 mm were placed in the liver slab to act as surgical clips for image registration. The slab was encased in Perspex to provide build up, and simulate the thoracic walls, with open ends to accommodate respiratory motion.

A cam drive system was installed to drive the respiratory motion, with the cam shaft attached to the lung slab and an electric motor used to rotate the cam. Voltage adjustment on the motor allows the user to change the speed and hence a range of breathing rates were achievable. The system provides a motion amplitude of 1.3 cm, giving a total displacement of 2.6 cm. A Perspex platform was attached to the base and connected to the cam drive system, allowing placement of a device to be tracked by the RPM infrared monitoring system for 4DCT acquisitions. The ion chamber cavity allows for placement of a Solid Water CC04 chamber insert in the liver slab, with effective point of measurement 2 cm from the lung–liver interface and at a central depth of 7 cm. The cavity was filled with Solid Water pieces when film is being measured or images acquired. Figure 1 shows the full phantom, while Fig. 2 demonstrates the location of the detectors, and Fig. 3 details the schematics.

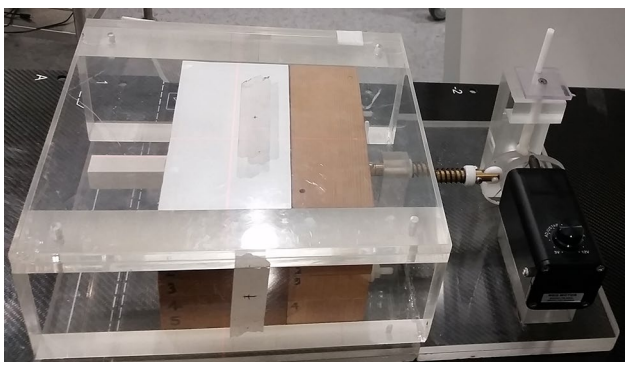

Fig. 1 Custom-made lung-liver respiratory phantom, designed and constructed by the NCCC

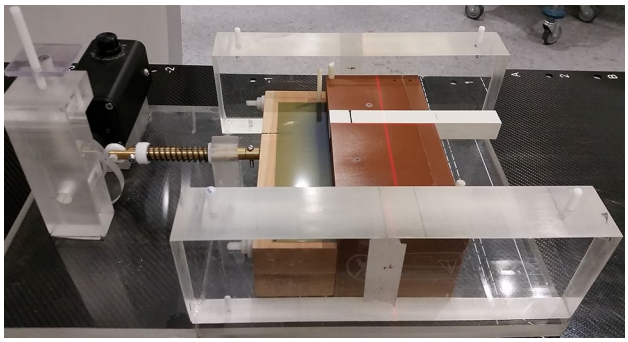

Fig. 2 Location of detector inserts for lung-liver respiratory phantom, with upper slices of material removed

Simulation and planning

A 4DCT image of the phantom was acquired on a Toshiba Aquilion LB scanner using the standard retrospective imaging protocol for 4D treatments, with slice thickness 3 mm. Data sets were acquired for breathing rates of 8, 14 and 23 breaths per minute (BPM), as well as a conventional 3D image with the phantom in the static exhale phase. There was found to be no discernible differences between the different breathing rates. An Elekta Monaco TPS was then used, under the guidance of an experienced planning therapist, to contour and plan on the exhale phase as per departmental protocol for 4D patients. The protocol includes adding a 6 mm expansion to the CTV for PTV creation and using specific beam templates and optimisation criteria starting points. Beam geometry is discussed below for each treatment technique. The single exhale phase is used for dosimetry as it is the only image type available on both the Monaco planning system and the Elekta linear accelerator (linac) kV imaging system (XVI). Processed images such as MIPs cannot be used for this purpose. The only CT dataset that is common (and therefore possible for use in patient alignment) for both the Elekta linac and the Monaco treatment planning system is the exhale phase. This is because the treatment plan that is linked with the CT data set (exhale phase) must be used for matching on the linac. The isocentre is thus placed at the centre of the clinical target volume (CTV) in the exhale phase, while the PTV (and the subsequent enclosing asymmetric field shape) is generated by summing the CTVs of each phase and adding an additional margin. Hence the results of this investigation are relevant to centres with the same planning and treatment equipment, that observe this limitation for 4D treatments.

Theoretical target volumes were developed based on data mined from previous liver SBRT patients treated within the department. Analysis revealed a median PTV volume of 60 cm^3 and average of 80 cm^3 for previous patients. As there is no physical 'tumour' present in the phantom, a theoretical spherical tumour volume was generated, with 2.6 cm of displacement in the superior–inferior direction, resulting in an elongated, capsule-shape clinical target volume. This

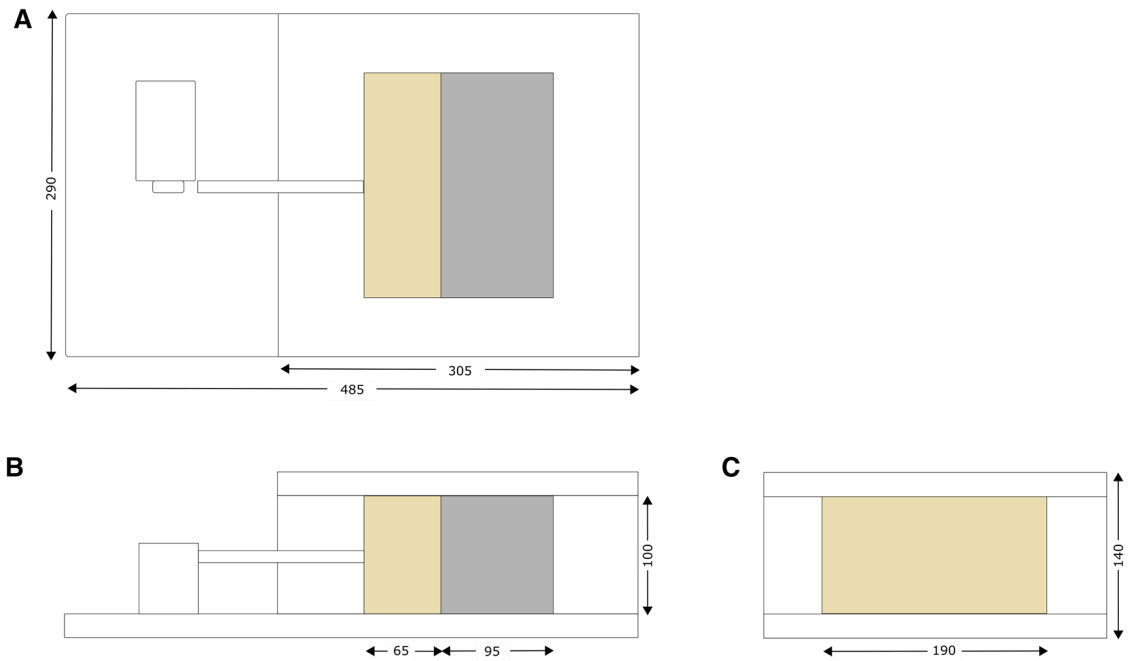

Fig. 3 Phantom schematics showing; **a** coronal view, **b** sagittal view and **c** transverse view, with lung material (yellow), liver material (grey) and location of the cam drive and motor (left). Units in mm

volume represents the final CTV which would be obtained on a patient 4D data set by summing the targets from each phase. An additional 6 mm uniform expansion margin was then added to the CTV to create a PTV of volume of 94.6 cm^3, which can adequately enclose the ionisation chamber sensitive volume. The CTV was placed near the lung–liver interface, hence the PTV extends several millimetres into the lung, which is where we expect the most significant deviations between calculated and measured results. Two generic organs at risk (OAR) contours were also generated adjacent to the PTV, to force modulation within the plans and more accurately replicate a clinical plan. OAR 1 had a total volume of 25.97 cm^3 and was located to the right of the PTV representing the duodenum, while OAR 2 had a volume of 17.70 cm^3 and was positioned posteriorly to the PTV, representing the spinal cord.

The Monaco Monte Carlo algorithm was used to calculate the dose for three treatment plans of different techniques on the same study set; static conformal (3DCRT), IMRT and VMAT plans. The plan prescription reflects current practice and was set as 4000 cGy in five fractions, resulting in a fractional dose of 800 cGy. 10 MV energy was used based on the treatment depth, grid size of 2 mm and statistical uncertainty of 1.00% per calculation. The 3DCRT plan used a six-beam isocentric arrangement chosen for delivery speed and to avoid critical structures. The fields were equally weighted and focused in the anterior and left directions to avoid the OAR structures. The VMAT plan was based on the current procedure for pelvic, 3D VMAT treatments. The plan was calculated with a single arc from gantry angle 180° rotating anticlockwise to 210°. The IMRT plan was developed with a seven-field, step and shoot technique and based on both clinical protocol and the existing VMAT plan. The IMRT constraints were the same as those used for VMAT, to allow a more direct comparison between the plans. A Monaco quality assurance (QA) plan was generated for each plan, to compare the fraction dose calculated to that delivered by the linac for point doses, and coronal 2D dose planes.

Ion chamber measurements

All measurements were performed on the same Elekta Axesse linac after a full machine warm up and output check. Point dose measurements were performed using an IBA CC04 ionisation chamber in a milled Solid Water insert and Unidos electrometer (PTW, Germany). Prior to taking phantom measurements, a set of reference readings were taken to convert the electrometer reading to absorbed dose. The readings were taken in a Solid Water phantom with 10 cm of backscatter to provide full scatter conditions and were re-taken after the phantom measurements to account for any changes to temperature, pressure or machine output. These readings were found to change by less than 0.1%. The phantom was then set up on the treatment couch and aligned to the laser markers in the exhale position and aligned using cone-beam CT (CBCT). Measurements were taken at isocentre, at a depth of 7 cm and distance 2 cm from the lung–liver interface. Readings were taken for each plan for the static case, and the three pre-determined breathing rates of 8, 14 and 23 bpm. For each case, a reading was taken when the phantom was at the inhale phase at the time of beam initiation, and a reading taken when the phantom was in the exhale phase during beam-on. The measured dose was compared to the Monaco calculated dose for each beam. The measurement uncertainty for the ion chamber experimentation was found to be 0.20% from repeat measurements in the static position.

Film measurements

Gafchromic EBT3 model 1417 film was used to measure 2D coronal dose planes for each treatment plan. Films of size of 10.3 cm × 14.0 cm were cut with the orientation maintained, along with calibration films for each set of measurements. All films were from the same batch. Each film was pre-scanned, flat on the glass of a film-dedicated EPSON Expression 10000XL scanner using a custom template, to assist with positional reproducibility and reduce excess light contributions. Calibration films were exposed immediately prior to the exposure of the treatment field films under reference conditions. The phantom was then placed on the couch, with the same set up as described above. A single film was placed within the phantom and isocentre marked on each edge using the linac crosshairs projection, with the orientation maintained. The film was located at depth 8 cm, 1 cm below the isocentre, but well within the PTV plane. Two films were then exposed for each of the three breathing rates and the static case; the first film exposed while the phantom was in the inferior, inhale position during beam-on (inhale measurement) and the second film exposed when the phantom was in the superior, exhale position (exhale measurement). This gives a total of eight films for each treatment plan.

All films were scanned and processed according to the protocol specified by Chung et al. [15]. Calibration films were used to determine sensitometric curves to relate the optical density to the absorbed dose for each pixel. The calibration curve was fitted to a rational function type as specified in the manufacturer's recommendations [16]. The uncertainty is approximately 4% in the clinical environment [15].

The film dose planes were compared to the Monaco calculated planes using Sun Nuclear Corporation's SNC Patient software (SNC, USA) to perform an absolute global gamma analysis using 3%, 3 mm criterion, with a lower dose threshold of 10%. A comparative analysis was also done between the inhale and exhale films for each breathing rate, and an

inter-comparison between the different breathing rates for each treatment plan. The film measured with the phantom in the static exhale position represents the actual planned geometry, and hence should give high gamma pass rates. 1D dose profiles were generated in the superior–inferior direction through the lateral isocentric position for each measured and calculated dose plane. Graphs were generated from the data for comparison showing the measured dose versus location in the superior–inferior plane. The location of the lung, liver and theoretical CTV are also shown on the graph to demonstrate the coverage of the CTV and effective of tissue heterogeneity on the dose distribution.

Results

A summary of the differences between the Monaco calculated point doses, and those measured with the ionisation chamber are found in Table 1. As expected, the smallest differences occur when the phantom is in the static exhale position, which represents the planned geometry. All plans showed good agreement with differences less than 1%, with IMRT showing the greatest discrepancy. This indicates the heterogeneities are well modelled by the TPS. Under motion, the differences between the doses at isocentre varied significantly. The conformal plan still showed agreement to within 1%, however the VMAT and IMRT plan had average deviations of up to 2.1%. VMAT showed a slightly higher average difference of 1.8%, measuring hotter than the calculated plan. IMRT had a similar difference of 1.6% but measured colder than the calculated plan. Interestingly, the signs are reversed in the static case for both modulated techniques. Higher variation in the calculated and measured point doses are expected for the modulated plans when compared to the 3DCRT plan due to beam segmentation. The modulated fields contain many small field segments, and steep dose gradients exist within the plans, hence small shifts from the point of measurement can result in large observed dose differences.

A summary of the dose plane comparisons with gamma analysis is located in Table 2. The gamma analysis pass rates are determined by the percentage of the total number of assessed points satisfying the 3% 3 mm criterion, and above the 10% threshold. The comparison between the Monaco calculated dose plane and the static exhale measurement film resulted in a pass rate of 97.6%, for 3DCRT, but only 94.0% for the VMAT plan. Analysis showed the TPS overestimated the dose in the low-dose region, while there was a region of hotter than expected points near the inferior PTV edge. The IMRT plan yielded a pass rate of 95.8%, lying between the VMAT and 3DCRT plans, with the TPS also underestimating the dose near the inferior PTV edge. There is a significant increase in the number of failing points when the phantom is in motion, with pass rates dropping to less than 50%. The films show the dose is stretched by approximately 2 cm in the superior–inferior direction for the motion cases. The failed points were predominantly located in the superior and inferior borders, with the superior region measuring much higher than calculated, and the inferior region measuring much lower than calculated. This is expected, because as the phantom moves to the inhale position the lung and liver move inferiorly. This causes the upper liver and lower lung to move into the field, and the lower liver region to move temporarily out of the field. An inter-comparison between the different cases, yielded pass rates greater than 94% for 3DCRT, indicating the technique is reproducible between different breathing rates and when beaming on at different stages of the respiratory cycle. VMAT resulted in the best consistency with pass rates greater than 95% for both treatments commencing at different breathing stages and different respiration rates. IMRT had the lowest agreement between different breathing rates but showed very little difference between beam-on time for the same breathing rate.

Table 1 Comparison of differences found between Monaco calculated point dose and results measured with ionisation chamber for each treatment technique

BPM	Start position	3DCRT % Difference	VMAT % Difference	IMRT % Difference
Static	Exhale	0.1	−0.3	0.9
14	Exhale	−0.3	1.5	−1.2
14	Inhale	−0.5	1.7	−1.4
23	Exhale	−0.4	1.4	−2.0
23	Inhale	−0.3	1.9	−1.8
8	Exhale	−0.3	2.0	−1.7
8	Inhale	−0.3	2.1	−1.6
Average	Non-static	−0.4	1.8	−1.6

Table 2 Comparison of both Monaco calculated dose plane, and film-measured dose planes using gamma analysis with 3%/3 mm criteria, for each treatment technique

Plane 1	Plane 2	Pass rate		
		3DCRT	VMAT	IMRT
Calculated	Static exhale meas.	97.6	94.0	95.8
8 bpm inhale meas.	8 bpm exhale meas.	98.5	95.3	92.5
14 bpm inhale meas.	14 bpm exhale meas.	94.1	99.8	99.5
23 bpm inhale meas.	23 bpm exhale meas.	99.4	97.3	91.3
14 bpm exhale meas.	8 bpm exhale meas.	99.8	95.0	99.8
14 bpm exhale meas.	23 bpm exhale meas.	99.6	96.0	99.6

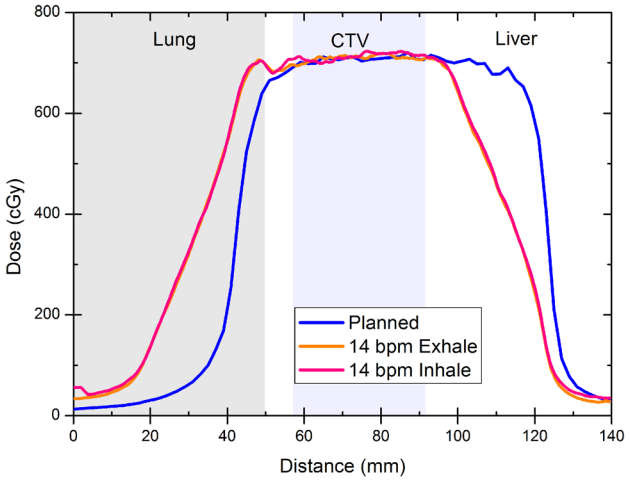

Fig. 4 1D comparison between the planned profile and measured 14 bpm profiles with the phantom starting on the exhale and inhale phase, for 3DCRT

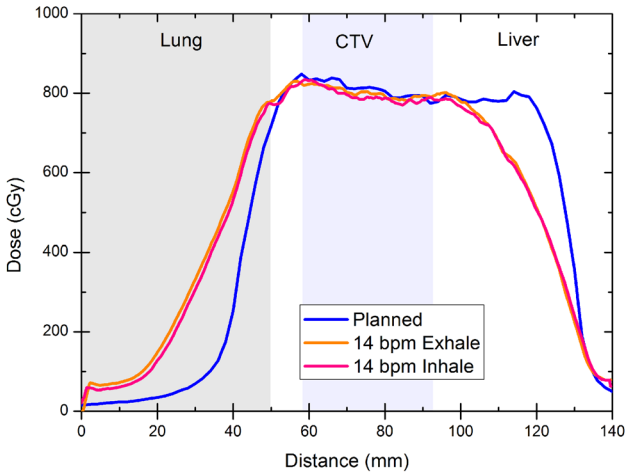

Fig. 6 1D comparison between the planned profile and measured 14 bpm profiles with the phantom starting on the exhale and inhale phase, for IMRT

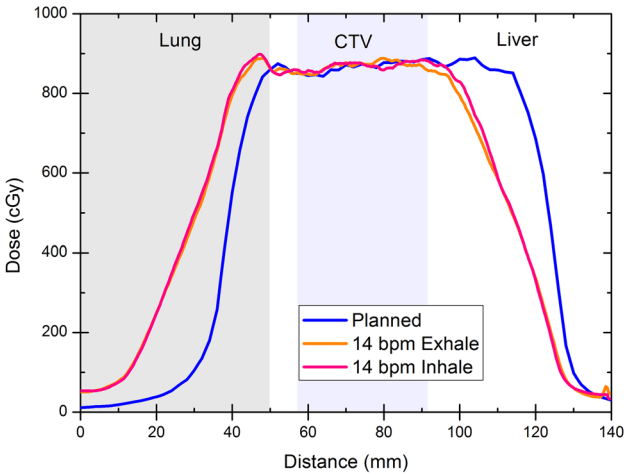

Fig. 5 1D comparison between the dose profile and measured 14 bpm profiles with the phantom starting on the exhale and inhale phase, for VMAT

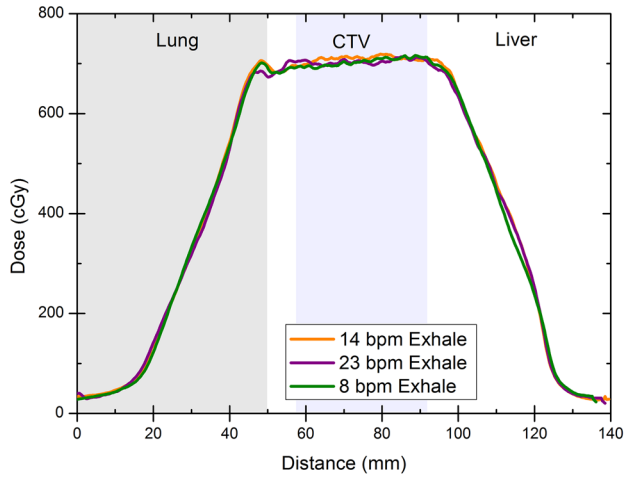

Fig. 7 1D comparison between the measured profiles for each breathing rate, starting in the exhale phase position, for 3DCRT

These variations indicate interplay may affect the delivery techniques differently.

Discussion

The 1D profiles were useful in demonstrating the CTV coverage in the superior–inferior direction for each plan, which is a key indicator of the technique suitability and whether planning margins are sufficient. Figures 4, 5 and 6 show a comparison between the calculated dose and measured 14 bpm profiles, with the phantom starting on both exhale and inhale phase. These graphs highlight the major limiting factor of the 4D planning protocol; plans are created on the exhale breathing phase only. This results in a systematic shift between the calculated dose distribution and measurement, with little consideration of the effect of moving tissue with very different electron densities. This however is a limitation, stated previously, due to the vendor software compatibility between Monaco and XVI image-guided radiation therapy (IGRT) system. The figures demonstrate that for each technique, the CTV is receiving the expected dose, and Figs. 7, 8 and 9 confirm this is upheld for all breathing rates. The field borders are less than 3 mm from the CTV edge, so while tis demonstrates the planning margins are sufficient, it also highlights the importance of respiratory motion management. If a patient's inspiration volume

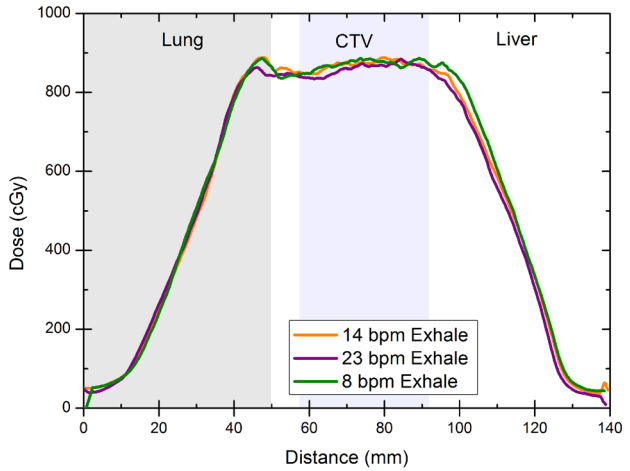

Fig. 8 1D comparison between the measured profiles for each breathing rate, starting in the exhale phase position, for VMAT

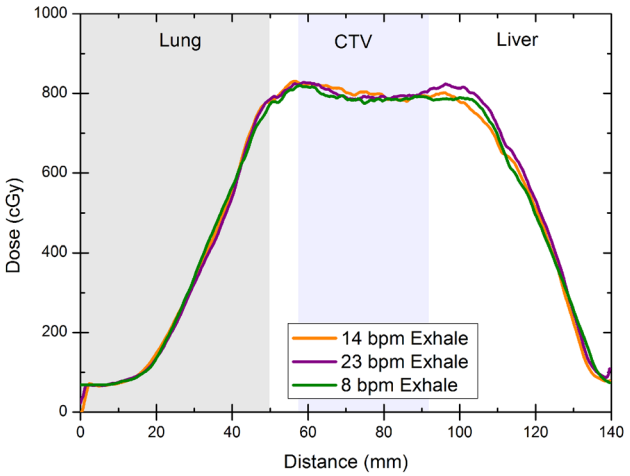

Fig. 9 1D comparison between the measured profiles for each breathing rate, starting in the exhale phase position, for IMRT

increases between simulation and treatment, the anatomy would be pushed more inferiorly and exceed the treatment margins. It is possible that part or all the CTV could move out of the treatment field, thus reducing the tumour coverage. The ABC system allows the treatment staff to monitor the expiration volume of the patient and interrupt the treatment field if the volume exceeds the limit determined during simulation, minimising this issue. The maximum dose and total lung volume irradiated are significantly higher than calculated, due to broadening of the penumbra, as shown by the profiles.

While the modulated technique shows little dosimetric advantage over the conformal techniques, VMAT has significantly faster delivery times, which is particularly important due to patient discomfort with arm positioning and respiratory management for this treatment type. Step and shoot IMRT however, has similar delivery times and requires patient plan verification. Although this technique could potentially be used for this treatment, VMAT appears to offer slightly superior dosimetric results, consistent with current trends within the department, where measured VMAT plans tend to have higher pass rates than IMRT plans when planned on the Monaco TPS. Thus, while 3DCRT will result in acceptable CTV coverage, VMAT appears to deliver a similar dosimetric outcome in a faster time, and the interplay effect appears to be minimal. The results agree with other studies which have shown that the use of intensity-modulated beams in upper abdomen sites introduces the interplay effect, which may offset the dosimetric advantages of IMRT and VMAT over conformal RT [17, 18]. Results from these studies also show however that the interplay effect appears to be minimised with fractionation, including SBRT techniques with a reduced number of fractions for lung lesions [19, 20].

It is important to note that this study only examines the interplay effect on dose distributions by varying the rate of respiration and position of target during beam on. These aspects were deemed the most likely to affect CTV coverage and were measurable with the tools available. Certain other variables that could affect the dose distribution including motion in the anterior–posterior direction, non-periodic motion, more complex and changing patient geometry and range of tumour motion were limited by the complexity of the respiratory phantom. Other aspects such as high dose rate, flattening filter-free deliveries were considered to have a potentially significant impact on the results however fell outside the scope of this study due to availability of a suitable beam model.

Conclusions

The use of conformal and intensity-modulated techniques in the treatment of HCC for different rates of respiration was evaluated. The disagreement between calculated and delivered point doses were within tolerances defined by the ICRU for conformal and intensity-modulated treatments [21, 22] for all three techniques. The CTV dose coverage was found to be adequate for the 3DCRT and VMAT techniques when under respiratory motion. Due to faster treatment times, a VMAT protocol is recommended to be implemented for treatments of HCC lesions adjacent to the diaphragm for free-breathing patients. The IMRT plan proved to be less reproducible than VMAT with poorer CTV coverage, was less robust against motion effects and requires equivalent treatment lengths to 3DCRT. Hence IMRT offers little to no dosimetric or treatment length advantage over 3DCRT, while requiring additional quality assurance.

The analysis of results also highlighted the importance of respiratory management during radiotherapy treatment to ensure optimal dose delivery to both the tumour volume and surrounding organs. Finally, the project demonstrated that both the 4D imaging and dosimetric outcomes were not significantly affected by the rate of respiration.

Acknowledgements The authors would like to thank Gordan Black for construction of the phantom, and the NCCC RTs for their support.

Compliance with ethical standards

Conflict of interest The authors declare that they have no conflicts of interest.

Ethical approval This article does not contain any studies with human participants or animals performed by any of the authors.

References

1. Habermehl D, Naumann P, Bendl R, Oelfke U, Nill S, Debus J, Combs SE (2015) Evaluation of inter- and intra-fractional motion of liver tumors using interstitial markers and implantable electromagnetic radiotransmitters in the context of image-guided radiotherapy (igrt)—the esmeralda trial. Radiat Oncol 10:1–5
2. Australian Institute of Health and Welfare (2017) Australian cancer incidence and mortality (ACIM) books: liver cancer. ACIM, Canberra
3. Dong P, Lee P, Ruan D, Long T, Romeijn E, Yang Y, Low D, Kupelian P, Shang K (2013) 4Pi non-coplanar liver SBRT: a novel delivery. Int J Radiat Oncol Biol Phys 85:1360–1366
4. Chen D, Wang R, Meng X, Liu T, Yan H, Feng R, Liu S, Jiang S, Xu X, Zhu K, Dou X (2014) A comparison of liver protection among 3-d conformal radiotherapy, intensity-modulated radiotherapy and rapidarc for hepatocellular carcinoma. Radiat Oncol 9:48
5. Xi M, Zhang L, Li QQ, Zhao L, Zhang R, Liu MZ (2013) Assessing the role of volumetric-modulated arc therapy in hepatocellular carcinoma. J Appl Clin Med Phys 14:81–90. https://doi.org/10.1120/jacmp.v14i3.4162
6. Guha C, Kavanagh BD (2011) Hepatic radiation toxicity: avoidance and amelioration. Semin Radiat Oncol 21(4):256–263
7. Benson A, D'Angelica M, Abrams T et al (2019) NCCN clinical practice guidelines in oncology: hepatobiliary cancers. Version 2.2019. National Comprehensive Cancer Network. https://www.nccn.org/professionals/physician_gls/pdf/hepatobiliary.pdf. Accessed 6 Mar 2019
8. Rim CH, Seong J (2016) Application of radiotherapy for hepatocellular carcinoma in current clinical practice guidelines. Radiat Oncol J 34:160–167
9. Head H, Dodd G, NC D, Prasad S, El-Merhi F, Freckleton M, Hubbard L (2007) Percutaneous radiofrequency ablation of hepatic tumours against the diaphragm: frequency of diaphragmatic injury. Radiology 243:877–884
10. Thomas E, Chapet O, Kessler ML, Lawrence TS, Haken RKT (2005) Benefit of using biological parameters (EUD and NTCP) in IMRT optimization for treatment of intrahepatic tumors. Int J Radiat Oncol Biol Phys 62:571–578
11. de Pooter JA, Romero AM, Wunderink W, Storchi PR, Heijmen BJ (2008) Automated non-coplanar beam direction optimization improves IMRT in SBRT of liver metastasis. Radiother Oncol 8:376–381
12. Bedos L, Riou O, Ailla res N, Braccini A, Molinier J, Llacer C (2016) Evaluation of reproducibility of tumor repositioning during multiple breathing cycles for liver stereotactic body radiotherapy treatment. Rep Pract Oncol Radiother 22(2):1507–1567. https://doi.org/10.1016/j.rpor.2016.07.007
13. Leibel S, Phillips T (2004) Textbook of radiation oncology, 2nd edition, Saunders, New York
14. Abbas H, Chang B, Chen ZJ (2004) Motion management in gastrointestinal cancers. J Gastrointest Oncol 5:223{235
15. Chung H, Lynch B, Samant S (2009) Chemiluminescence of Renilla (sea pansy) luciferin and its analogues. J Chem Soc Chem Commun. https://doi.org/10.1039/C39730000492
16. Ashland (2017) GAFCHROMIC Dosimetry Media, Type EBT3. http://www.gafchromic.com/documents/EBT3_Specifications.pdf. Accessed 12 Nov 2018
17. Yoganathan SA, Maria Das KJ, Agarwal A, Kumar S (2017) Magnitude, impact, and management of respiration-induced target motion in radiotherapy treatment: a comprehensive review. J Med Phys 42(3):101–115
18. Bortfeld T, Jokivarsi K, Goitein M, Kung J, Jiang SB (2002) Effects of intra-fraction motion on IMRT dose delivery: statistical analysis and simulation. Phys Med Biol 47:2203–2220
19. Li X, Yang Y, Li T, Fallon K, Heron DE, Huq MS et al (2013) Dosimetric effect of respiratory motion on volumetric-modulated arc therapy-based lung SBRT treatment delivered by trueBeam machine with flattening filter-free beam. J Appl Clin Med Phys 14:4370
20. Ong C, Verbakel WF, Cuijpers JP, Slotman BJ, Senan S (2011) Dosimetric impact of interplay effect on rapidArc lung stereotactic treatment delivery. Int J Radiat Oncol Biol Phys 79:305–311
21. Landberg T, Chavaudra J, Dobbs J, Gerard JP, Hanks G, Horiot JC, Johansson KA, Möller T, Purdy J, Suntharalingam N, Svensson H (1999) Report 62, J Int Comm Radiat Units Meas. https://doi.org/10.1093/jicru/os32.1.Report62
22. (2010) Report 83. J Int Comm Radiat Units Meas. https://doi.org/10.1093/jicru/10.1.Report83